Noname manuscript No.
(will be inserted by the editor)

Wendland functions with increasing smoothness converge to a Gaussian

A. Chernih · I. H. Sloan · R. S. Womersley

arXiv:1203.5696v2 [math.NA] 16 May 2012

the date of receipt and acceptance should be inserted later

March 1, 2013

Abstract The Wendland functions are a class of compactly supported radial basis functions with a user-specified smoothness parameter. We prove that with an appropriate rescaling of the variables, both the original and the "missing" Wendland functions converge uniformly to a Gaussian as the smoothness parameter approaches infinity. We also give numerical experiments with Wendland functions of different smoothness.

Keywords Radial basis functions · compact support · smoothness · Wendland functions · Gaussian.

Mathematics Subject Classification (2010) 33C90 · 41A05 · 41A15 · 41A30 · 41A63 · 65D07 · 65D10

1 Introduction

In recent years radial basis functions (RBFs) have become a popular tool for scattered data approximation and interpolation and for solving partial differential

---

This work was supported by the Australian Research Council. The authors thank Holger Wendland, Robert Schaback and Simon Hubbert for helpful discussions.

A. Chernih
School of Mathematics and Statistics, University of New South Wales, Sydney NSW 2052, Australia
Tel.: +61-410-697411, Fax: +612 93857123
E-mail: andrew@andrewch.com

I. H. Sloan
School of Mathematics and Statistics, University of New South Wales
E-mail: i.sloan@unsw.edu.au

R. S. Womersley
School of Mathematics and Statistics, University of New South Wales
E-mail: r.womersley@unsw.edu.au

equations. Two excellent recent books covering practical and theoretical issues are Fasshauer [6] and Wendland [18]. A function $\Phi : \mathbb{R}^d \to \mathbb{R}$ is said to be *radial* if there exists a function $\phi : [0, \infty) \to \mathbb{R}$ such that $\Phi(\mathbf{x}) = \phi(\|\mathbf{x}\|_2)$ for all $\mathbf{x} \in \mathbb{R}^d$. Then we can define an RBF for a given centre $\mathbf{x}_i \in \mathbb{R}^d$ as

$$\Phi_i(\mathbf{x}) = \phi(\|\mathbf{x} - \mathbf{x}_i\|_2).$$

For example, an interpolant $\mathcal{I}$ for the scattered data interpolation problem, where we are given data $(\mathbf{x}_j, y_j), j = 1, \ldots, n$, with $\mathbf{x}_j \in \mathbb{R}^d$ and $y_j \in \mathbb{R}$, can be constructed as the linear combination

$$\mathcal{I}(\mathbf{x}) = \sum_{i=1}^{n} c_i \Phi_i(\mathbf{x}), \quad \mathbf{x} \in \mathbb{R}^d, \tag{1}$$

where the coefficients $c_1, \ldots, c_n$ are chosen so that

$$\mathcal{I}(\mathbf{x}_j) = y_j, \quad j = 1, \ldots, n. \tag{2}$$

If Φ is positive definite, then (1) and (2) have a unique solution. We recall that a continuous function $f : \mathbb{R}^d \to \mathbb{R}$ is *positive definite* (some would say *strictly positive definite*) if for any n distinct points $\mathbf{x}_1, \ldots, \mathbf{x}_n \in \mathbb{R}^d$, the quadratic form

$$\sum_{i=1}^{n} \sum_{j=1}^{n} \alpha_i \alpha_j \, f(\mathbf{x}_i - \mathbf{x}_j)$$

is positive for all $\boldsymbol{\alpha} = [\alpha_1, \ldots, \alpha_n]^T \in \mathbb{R}^n \backslash \{\mathbf{0}\}$.

Most geophysical applications are in $\mathbb{R}^3$, but in other areas, such as machine learning, different spatial dimensions may occur (see, for example, [3]).

Broadly speaking RBFs can be categorised as either *globally supported* or *compactly supported*. The first category includes Gaussians and multiquadrics [6]. Both have a scale parameter (also known as a shape or tension parameter), the selection of which is still a major ongoing research topic.

The second category includes Wendland functions [17], Buhmann RBFs [4], Wu's RBFs [19] and "Euclid's hat" [8,13]. The most widely used in this category are the Wendland functions, which are piecewise polynomial compactly supported functions. They have the minimum polynomial degree for any level of smoothness, and have a strictly positive Fourier transform. The Wendland functions were originally derived for integer-order Sobolev spaces in odd dimensions in Wendland [17] and were then extended to even dimensions in Schaback [14] (Schaback called these the "missing" Wendland functions). They are uniquely defined for a given spatial dimension d and a smoothness parameter k (up to a constant multiplier). All the Wendland functions are equal to zero outside [0,1].

Our purpose in this paper is to consider the limiting case of both the original and the missing Wendland functions as the smoothness parameter k goes to infinity. In Figure 1, we can see the original Wendland functions in $\mathbb{R}^3$ for $k = 1, \ldots, 5$, where we have normalised the functions to have value 1 at the origin. One can clearly see faster decay as k increases, which suggests the need for a change of variable when considering the limit as k approaches infinity. In Section 2 we give some necessary background on radial basis functions and Fourier transforms. Then in Section 3 we define the Wendland functions $\phi_{\ell,k}$, where k is a non-negative integer for the original Wendland functions and a positive half-integer for the missing Wendland functions. We also define *normalised Wendland functions* $\tilde{\phi}_{\ell,k}$ and *normalised equal area Wendland functions* $\psi_{\ell,k}$, where the latter are obtained by a linear change of scale in the argument so as to ensure equal areas under their graphs for all values of k. In Section 4 we consider the limit of the normalised equal area Wendland functions as the smoothness parameter goes to infinity. Our main theorem is Theorem 4.3, which states that the normalised equal area Wendland functions converge uniformly to a Gaussian on the real half-line. Section 5 provides numerical evidence to illustrate the theoretical results, as well as an example of interpolation using the normalised Wendland functions and the normalised equal area Wendland functions. This example compares results obtained with the Wendland functions of different smoothness as well as the limiting Gaussian. The results of the experiment show only small differences in errors when using normalised equal area Wendland functions with different smoothness parameters, but the condition number of the linear system grows quickly as the smoothness parameter increases. A cautious conclusion might be that there is little incentive to consider using high values for the smoothness parameter.

We note that the similarity of the normalised Wendland functions to a Gaussian has been mentioned in [11] and of the normalised equal area Wendland functions to a Gaussian in [7], in both cases for $\mathbb{R}^3$ with $k = 1$. No theoretical explanations were given for these observations.

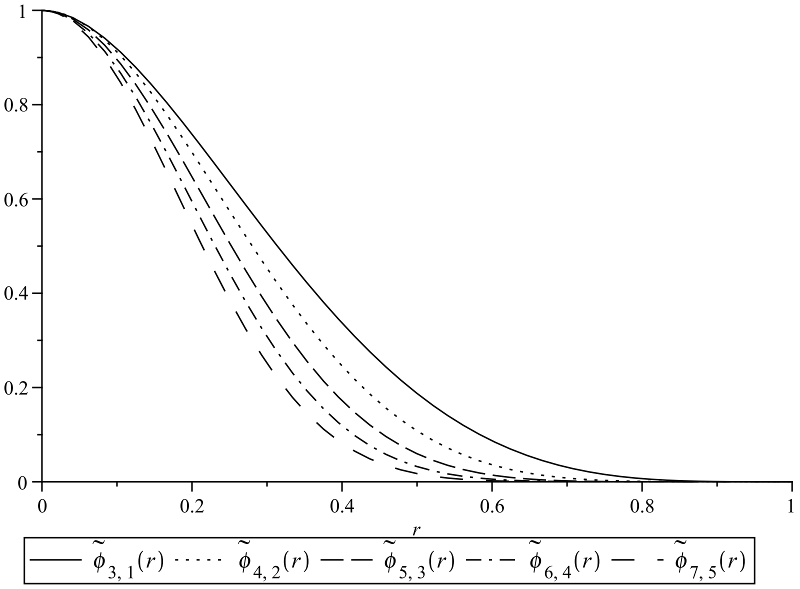

Fig. 1: The (original) Wendland functions $\tilde{\phi}_{3,1}(r)$, $\tilde{\phi}_{4,2}(r)$, $\tilde{\phi}_{5,3}(r)$, $\tilde{\phi}_{6,4}(r)$ and $\tilde{\phi}_{7,5}(r)$ normalised to have value 1 at $r = 0$.

2 Background

In this section, we will provide background material on several types of radial basis functions, the Fourier transform and the inverse Fourier transform.

2.1 Wendland functions

Wendland functions were originally introduced in [17] and then more cases were added in [14]. We will refer to the Wendland functions from [17] as the *original Wendland functions* and the Wendland functions from [14] as the *missing Wendland functions*. A thorough investigation of both types of Wendland functions in terms of hypergeometric functions and other special functions is the focus of Hubbert [10]. We firstly define the original and missing Wendland functions and then discuss the properties of each.

Definition 2.1 *With spatial dimension d, smoothness parameter $k > 0$, and $\ell := \lfloor \frac{d}{2} + k \rfloor + 1$, let*

$$\phi_{\ell,k}(r) := \begin{cases} \dfrac{1}{\Gamma(k)\, 2^{k-1}} \displaystyle\int_r^1 s\,(1-s)^{\ell}(s^2 - r^2)^{k-1} \mathrm{d}s & \text{for} \quad 0 \le r \le 1, \\ 0 & \text{for} \quad r > 1. \end{cases} \tag{3}$$

This defines the original Wendland functions when k is a positive integer and the missing Wendland functions when k is a positive half-integer.

Both the original Wendland functions and the missing Wendland functions are continuous on $[0, \infty)$. Note that this choice of ℓ is the minimum value that ensures that the resulting functions are positive definite. Since $\ell = \lfloor \frac{d}{2} + k \rfloor + 1$ it follows immediately that for fixed d

$$\ell \sim k \text{ as } k \to \infty, \tag{4}$$

where $x \sim y$ denotes asymptotic equality, that is $\frac{x}{y} \to 1$. If we wish to use a different support, this can be easily achieved through scaling the function argument: if $\phi(r)$ has support $[0, 1]$ then with the change of variable $y = \delta\, r$, $\psi(y) := \phi\left(\frac{y}{\delta}\right)$ has support $[0, \delta]$.

The original Wendland functions are constructed with the minimal degree polynomial for a given smoothness that gives rise to a d-dimensional positive definite function. They are unique up to a multiplicative constant when $k > 0$. Another important property is that for an odd space dimension d and for k a non-negative integer the function

$$K(\mathbf{x}, \mathbf{y}) = \phi_{\ell,k}(\|\mathbf{x} - \mathbf{y}\|), \quad \mathbf{x}, \mathbf{y} \in \mathbb{R}^d, \tag{5}$$

is the reproducing kernel of a Hilbert space which is norm equivalent to the Sobolev space $H^{\frac{d+1}{2}+k}(\mathbb{R}^d)$ [18, Chapter 10].

We give explicit formulae for the original Wendland functions for $d = 3$ and $k = 1, 2, \ldots, 5$ in Table 1 where $\doteq$ denotes equality up to a positive constant factor. The support of all the original Wendland functions is $[0, 1]$.

k	Original Wendland function
1	$\phi_{3,1}(r) \doteq (1-r)_+^4(4r+1)$
2	$\phi_{4,2}(r) \doteq (1-r)_+^6(35r^2+18r+3)$
3	$\phi_{5,3}(r) \doteq (1-r)_+^8(32r^3+25r^2+8r+1)$
4	$\phi_{6,4}(r) \doteq (1-r)_+^{10}(429r^4+450r^3+210r^2+50r+5)$
5	$\phi_{7,5}(r) \doteq (1-r)_+^{12}(2048r^5+2697r^4+1644r^3+566r^2+108r+9)$

Table 1: The original Wendland functions $\phi_{\ell,k}(r)$ for $d = 3$ and $k = 1, \ldots, 5$.

Schaback [14] extended Wendland's original approach to cover the missing Wendland functions, which are the reproducing kernels of integer order Sobolev spaces in even dimensions d. An important distinction between the original Wendland functions and the missing Wendland functions is that the missing Wendland functions, whilst still being compactly supported, now have logarithmic and square-root multipliers of polynomial components. We give explicit formulae for the missing Wendland functions for $d = 2$ and $k = \frac{1}{2}, \frac{3}{2}$ and $\frac{5}{2}$ in Table 2. The support of all the missing Wendland functions is $r \in [0, 1]$, while

$$L(r) := \log\left(\frac{r}{1+\sqrt{1-r^2}}\right) \quad \text{and} \quad S(r) := \sqrt{1-r^2}.$$

It is proved in [14] that with $\ell = \lfloor \frac{d}{2} + k \rfloor + 1$ and k being any positive half-integer,

k	Missing Wendland function
$\frac{1}{2}$	$\phi_{2,\frac{1}{2}}(r) \doteq 3r^2L(r) + (2r^2+1)S(r)$
$\frac{3}{2}$	$\phi_{3,\frac{3}{2}}(r) \doteq 15r^4(6+r^2)L(r) + (81r^4+28r^2-4)S(r)$
$\frac{5}{2}$	$\phi_{4,\frac{5}{2}}(r) \doteq (945r^8+2520r^6)L(r) + (256r^8+263r^6+690r^4-136r^2+16)S(r)$

Table 2: The missing Wendland functions $\phi_{\ell,k}(r)$ for $d = 2$ and $k = \frac{1}{2}, \frac{3}{2}, \frac{5}{2}$.

for an even dimension d the kernel in (5) is the reproducing kernel of a Hilbert space that is norm equivalent to the Sobolev space $H^{\frac{d+1}{2}+k}(\mathbb{R}^d)$.

Hereafter when we refer to *Wendland functions* we will mean both the original and missing Wendland functions. They will both be denoted by $\phi_{\ell,k}(r)$ where

$$\ell = \left\lfloor \frac{d}{2} + k \right\rfloor + 1$$

and $r \in [0,1]$, with k an integer for the original Wendland functions and a half-integer for the missing Wendland functions.

2.2 Fourier transforms

The proofs of the main results rely heavily on Fourier transforms. This section provides definitions and outlines some key properties. For further information, we refer the interested reader to [15, 18].

With the Fourier transform of $f \in L_1(\mathbb{R}^d)$ defined as

$$\widehat{f}(\mathbf{w}) := (2\pi)^{-\frac{d}{2}} \int_{\mathbb{R}^d} f(\mathbf{x})\, e^{-i\mathbf{w}\cdot\mathbf{x}}\, \mathrm{d}\mathbf{x}, \quad \mathbf{w} \in \mathbb{R}^d,$$

it is well known that the Fourier transform of a radial function $\Phi \in L_1(\mathbb{R}^d) \cap C(\mathbb{R}^d)$ is also radial and is given by $\widehat{\Phi}(\mathbf{w}) = \mathcal{F}_d\phi(\|\mathbf{w}\|_2)$ where

$$\mathcal{F}_d\phi(z) := z^{1-\frac{d}{2}} \int_0^\infty \phi(y)\, y^{\frac{d}{2}}\, J_{\frac{d}{2}-1}(z\,y)\, \mathrm{d}y, \tag{6}$$

and $J_\nu(y)$ denotes the Bessel function of the first kind with order ν.

From the Fourier inversion theorem applied to radial functions, we know that if $\Phi \in L_1(\mathbb{R}^d)$ with $\Phi(\mathbf{x}) = \phi(\|\mathbf{x}\|_2)$, $\phi : [0,\infty) \to \mathbb{R}$, and if $\widehat{\Phi} \in L_1(\mathbb{R}^d)$, then

$$\phi(y) = y^{1-\frac{d}{2}} \int_0^\infty \mathcal{F}_d\phi(z)\, z^{\frac{d}{2}}\, J_{\frac{d}{2}-1}(yz)\, \mathrm{d}z. \tag{7}$$

We also recall that if $f \in L_1(\mathbb{R}^d) \cap C(\mathbb{R}^d)$ is positive definite then its Fourier transform is in $L_1(\mathbb{R}^d)$ and is non-negative [18, Corollary 6.12].

The Gaussian radial basis function with scale parameter $\alpha > 0$, which we denote by $G_\alpha(y)$, is given by

$$G_\alpha(y) := e^{-\alpha\, y^2}, \quad y \in \mathbb{R},$$

and its Fourier transform is given by

$$\widehat{G}_\alpha(z) = \frac{1}{(2\alpha)^{\frac{d}{2}}}\, e^{-\frac{z^2}{4\alpha}}, \quad z \in \mathbb{R}.$$

We will first define the generalised hypergeometric function and then state the Fourier transform of the Wendland functions. Further details on generalised hypergeometric functions can be found in [1] and [2].

Definition 2.2 *The generalised hypergeometric function ${}_pF_q(a_1, \ldots, a_p; b_1, \ldots, b_q; x)$ is*

$${}_pF_q(a_1, \ldots, a_p; b_1, \ldots, b_q; x) := \sum_{n=0}^{\infty} \frac{(a_1)_n \cdots (a_p)_n}{(b_1)_n \cdots (b_q)_n} \frac{x^n}{n!},$$

where none of $b_1, \ldots, b_q$ is a negative integer or zero and where

$$(c)_n := c(c+1)\cdots(c+n-1) = \frac{\Gamma(c+n)}{\Gamma(c)}, \quad n \geq 1 \tag{8}$$

denotes the Pochhammer symbol, with $(c)_0 = 1$. *When* $p \leq q$ *the series converges for all finite* x *and defines an entire function. When* $p = q + 1$ *the series converges absolutely for* $|x| < 1$, *and also at* $x = 1$ *if*

$$\sum_{i=1}^{q} b_i - \sum_{i=1}^{p} a_i > 0.$$

Theorem 2.3 *The d-dimensional Fourier transform of* $\phi_{\ell,k}$ *is given by*

$$\mathcal{F}_d \phi_{\ell,k}(z) = C_d^{\ell,k} {}_1F_2 \left(\frac{d+1}{2} + k; \frac{\ell+d+1}{2} + k, \frac{\ell+d+2}{2} + k; -\frac{z^2}{4} \right), \quad z > 0,$$

where

$$C_d^{\ell,k} := \frac{2^{k+\frac{d}{2}} \Gamma(\ell+1) \Gamma\left(\frac{d+1}{2} + k\right)}{\sqrt{\pi} \Gamma(\ell + d + 2k + 1)}.$$

Proof This result can be found in [20], however for completeness, we provide it here in more detail. With (3) and (6) and with the change of variables $s = y/t$ and $x = t$ in the second line, we have that

$$\begin{aligned} \mathcal{F}_d \phi_{\ell,k}(z) &= \frac{z^{1-\frac{d}{2}}}{2^{k-1}\Gamma(\alpha)} \int_0^1 \int_y^1 (1-t)^\ell \, t \left(t^2 - y^2\right)^{k-1} y^{\frac{d}{2}} J_{\frac{d}{2}-1}(zy) \, \mathrm{d}t \, \mathrm{d}y \\ &= \frac{z^{1-\frac{d}{2}}}{2^{k-1}\Gamma(k)} \int_0^1 \int_0^1 x^{2k+\frac{d}{2}} (1-x)^\ell \, s^{\frac{d}{2}} \left(1 - s^2\right)^{k-1} J_{\frac{d}{2}-1}(zsx) \, \mathrm{d}s \, \mathrm{d}x. \end{aligned}$$

From [9, 6.567.1], we have that

$$\int_0^1 x^{\nu+1} \left(1 - x^2\right)^\mu J_\nu(bx) \, \mathrm{d}x = 2^\mu \Gamma(\mu+1) b^{-(\mu+1)} J_{\nu+\mu+1}(b), b > 0,$$

which means we can simplify our expression to

$$\mathcal{F}_d \phi_{\ell,k}(z) = z^{1-\frac{d}{2}} \int_0^1 x^{k+\frac{d}{2}} (1-x)^\ell J_{k+\frac{d}{2}-1}(zx) \, \mathrm{d}x.$$

With the following identity [9, 6.569]

$$\begin{aligned} \int_0^1 x^\lambda (1-x)^{\mu-1} J_\nu(ax) \, \mathrm{d}x &= \frac{\Gamma(\mu)\Gamma(\lambda+\nu+1) 2^{-\nu} a^\nu}{\Gamma(\nu+1)\Gamma(\lambda+\mu+\nu+1)} \\ \times {}_2F_3 &\left(\frac{\lambda+\nu+1}{2}, \frac{\lambda+\nu+2}{2}; \nu+1, \frac{\lambda+\nu+\mu+1}{2}, \frac{\lambda+\nu+\mu+1}{2}; -\frac{z^2}{4} \right), \end{aligned}$$

the result follows after applying the duplication formula for the gamma function [1, 6.1.18]

$$\Gamma(z) \Gamma\left(z + \frac{1}{2}\right) = 2^{1-2z} \sqrt{\pi} \, \Gamma(2z), \tag{9}$$

and noting that in our case, the ${}_2F_3$ hypergeometric function simplifies down to a ${}_1F_2$ since the first parameters in the numerator and denominator are equal.

3 Normalised and normalised equal area Wendland functions

Hubbert [10] starts with the integral representation (3) to express the Wendland functions in terms of Legendre functions. Equation (3.4) in [10] states that for $r \in (0,1]$

$$\phi_{\ell,k}(r) = \frac{\Gamma(\ell+1)}{2^{\ell+k}\Gamma(\ell+k+1)}\,(1-r^2)^{\ell+k} r^{-\ell}{}_2F_1\left(\frac{\ell}{2}, k+\frac{\ell+1}{2}; \ell+k+1; 1-\frac{1}{r^2}\right). \tag{10}$$

Now we apply the following identity [1, 15.3.4]

$${}_2F_1(a,b;c;z) = (1-z)^{-a}{}_2F_1\left(a, c-b; c; \frac{z}{z-1}\right) \tag{11}$$

to (10), which gives us, for $r \in [0,1]$, (since we recover the case of $r = 0$ by right continuity)

$$\phi_{\ell,k}(r) = \frac{\Gamma(\ell+1)}{2^{\ell+k}\Gamma(\ell+k+1)}(1-r^2)^{\ell+k}{}_2F_1\left(\frac{\ell}{2}, \frac{\ell+1}{2}; \ell+k+1; 1-r^2\right). \tag{12}$$

We will need the *normalised* Wendland functions, which we denote by $\tilde{\phi}_{\ell,k}(r)$, where

$$\tilde{\phi}_{\ell,k}(r) := \frac{\phi_{\ell,k}(r)}{\phi_{\ell,k}(0)}, \tag{13}$$

so that $\tilde{\phi}_{\ell,k}(0) = 1$.

Theorem 3.1

$$\tilde{\phi}_{\ell,k}(r) = \begin{cases} \frac{(2k)_{\ell+1}}{(k)_{\ell+1}}\,\frac{1}{2^{\ell+1}}\,(1-r^2)^{\ell+k}\,{}_2F_1\left(\frac{\ell}{2}, \frac{\ell+1}{2}; \ell+k+1; 1-r^2\right) & 0 \le r \le 1, \\ 0 & r > 1. \end{cases} \tag{14}$$

Proof To calculate $\phi_{\ell,k}(0)$ we need the value of the hypergeometric function in (12) at the argument 1 (since it has argument $1-r^2$). From [1, 15.1.20] we have the identity

$${}_2F_1(a,b;c;1) = \frac{\Gamma(c)\Gamma(c-b-a)}{\Gamma(c-b)\Gamma(c-a)} \quad , \quad c-b-a > 0. \tag{15}$$

Applying (15) to (12) shows that

$$\phi_{\ell,k}(0) = \frac{\Gamma(\ell+1)\,\Gamma(k+\frac{1}{2})}{2^{\ell+k}\,\Gamma(\frac{\ell}{2}+k+\frac{1}{2})\,\Gamma(\frac{\ell}{2}+k+1)}.$$

Using (9) twice – firstly for $\Gamma(\frac{\ell}{2}+k+\frac{1}{2})\Gamma(\frac{\ell}{2}+k+1)$ and then for $\Gamma(k)\Gamma\left(k+\frac{1}{2}\right)$ – and with several terms cancelling out in the numerator and denominator, we get

$$\phi_{\ell,k}(0) = \frac{\Gamma(\ell+1)\Gamma(2k)}{2^{k-1}\Gamma(k)\Gamma(\ell+2k+1)}. \tag{16}$$

Now using (12) and (16) we can see that for $r \in [0,1]$

$$\tilde{\phi}_{\ell,k}(r) = \frac{\Gamma(k)\Gamma(\ell+2k+1)}{\Gamma(2k)\Gamma(\ell+k+1)} \frac{1}{2^{\ell+1}} (1-r^2)^{\ell+k} {}_2F_1\left(\frac{\ell}{2}, \frac{\ell+1}{2}; \ell+k+1; 1-r^2\right)$$

which coincides with (14). □

We will also need the following result for the area under the Wendland functions.

Lemma 3.2 *The area under the graph of $\phi_{\ell,k}(r), r \geq 0$, is*

$$a_{\ell,k} = \frac{2^k\, \Gamma(\ell+1)\, \Gamma(k+1)}{\Gamma(\ell+2k+2)}. \tag{17}$$

Proof Since the Wendland function is equal to zero for $r > 1$ we need consider only the integral over $[0,1]$. Then

$$\begin{aligned} a_{\ell,k} &= \int_0^1 \phi_{\ell,k}(r)\,\mathrm{d}r && (18)\\ &= \frac{\Gamma(\ell+1)}{2^{\ell+k}\Gamma(\ell+k+1)} \int_0^1 (1-r^2)^{\ell+k} {}_2F_1\left(\frac{\ell}{2}, \frac{\ell+1}{2}; \ell+k+1; 1-r^2\right) \mathrm{d}r \\ &= \frac{\Gamma(\ell+1)}{2^{\ell+k+1}\Gamma(\ell+k+1)} \int_0^1 y^{\ell+k}\, (1-y)^{-\frac{1}{2}} {}_2F_1\left(\frac{\ell}{2}, \frac{\ell+1}{2}; \ell+k+1; y\right) \mathrm{d}y \\ &=: \frac{\Gamma(\ell+1)}{2^{\ell+k+1}\Gamma(\ell+k+1)} I_{\ell,k}, && (19) \end{aligned}$$

by using (12) in the second line, the substitution $y = 1 - r^2$ in the third line and defining $I_{\ell,k}$ as the integral in the third line. Using the identity [1, 15.3.3]

$${}_2F_1(a,b;c;z) = (1-z)^{c-a-b}\, {}_2F_1(c-a, c-b; c; z), \tag{20}$$

we can rewrite $I_{\ell,k}$ as

$$I_{\ell,k} = \int_0^1 y^{\ell+k}\, (1-y)^k\, {}_2F_1\left(\frac{\ell}{2}+k+1, \frac{\ell}{2}+k+\frac{1}{2}; \ell+k+1; y\right) \mathrm{d}y. \tag{21}$$

Now we can use the identity [9, 7.512(4)]

$$\int_0^1 x^{\gamma-1}\, (1-x)^{\rho-1}\, {}_2F_1\left(\alpha, \beta; \gamma; x\right) \mathrm{d}x = \frac{\Gamma(\gamma)\Gamma(\rho)\Gamma(\gamma+\rho-\alpha-\beta)}{\Gamma(\gamma+\rho-\alpha)\Gamma(\gamma+\rho-\beta)}, \tag{22}$$

which is valid for $\mathrm{Re}\ \gamma > 0, \mathrm{Re}\ \rho > 0$ and $\mathrm{Re}(\gamma+\rho-\alpha-\beta) > 0$. With $\gamma = \ell+k+1$, $\rho = k+1$, $\alpha = \frac{\ell}{2}+k+1$ and $\beta = \frac{\ell+1}{2}+k$ and noting that $\Gamma\left(\frac{1}{2}\right) = \sqrt{\pi}$, we get

$$I_{\ell,k} = \frac{\Gamma(\ell+k+1)\Gamma(k+1)\sqrt{\pi}}{\Gamma\left(k+\frac{\ell}{2}+1\right)\Gamma\left(k+\frac{\ell}{2}+\frac{3}{2}\right)}. \tag{23}$$

Then using (9) and substituting (23) into (19) we get (17). □

Now we can define what we will call *normalised equal area Wendland functions*. These are normalised Wendland functions with a linear change of variable (which depends on k and a positive real constant α) such that for a given α all the normalised equal area Wendland functions have area equal to the area under $\exp(-\alpha y^2)$ over the real half-line. The value of α can be chosen for the convenience of the user. We will denote the normalised equal area Wendland functions by $\psi_{\ell,k}$.

Theorem 3.3 *With α any positive real constant and*

$$\delta_{\ell,k}(\alpha) := \frac{(\ell+2k+1)\,\Gamma\left(k+\frac{1}{2}\right)}{2\sqrt{\alpha}\,\Gamma(k+1)}, \tag{24}$$

the normalised equal area Wendland functions

$$\psi_{\ell,k}(y) := \begin{cases} \tilde{\phi}_{\ell,k}\left(\frac{y}{\delta_{\ell,k}(\alpha)}\right) & \text{for} \quad 0 \le y \le \delta_{\ell,k}(\alpha), \\ 0 & \text{for} \quad y > \delta_{\ell,k}(\alpha) \end{cases} \tag{25}$$

have area under the graph equal to $\frac{1}{2}\sqrt{\pi/\alpha}$, the area under $\exp(-\alpha y^2)$ over the real half-line.

Proof With (17) and (16), we can see this as follows

$$\begin{aligned} \int_0^{\delta_{\ell,k}(\alpha)} \tilde{\phi}_{\ell,k}\left(\frac{y}{\delta_{\ell,k}(\alpha)}\right) \mathrm{d}y &= \delta_{\ell,k}(\alpha) \int_0^1 \tilde{\phi}_{\ell,k}(r)\,\mathrm{d}r \\ &= \frac{\delta_{\ell,k}(\alpha)}{\phi_{\ell,k}(0)} \int_0^1 \phi_{\ell,k}(r)\,\mathrm{d}r \\ &= \frac{\delta_{\ell,k}(\alpha)}{\phi_{\ell,k}(0)} a_{\ell,k} \\ &= \frac{\sqrt{\pi}}{2\sqrt{\alpha}} \\ &= \int_0^\infty \exp(-\alpha y^2)\,\mathrm{d}y. \end{aligned}$$

□

In Figure 2 we plot the normalised equal area Wendland functions $\psi_{\ell,k}$ for $k = 1, \ldots, 5$ with $\alpha = 1$.

We emphasise that the normalised equal area Wendland functions satisfy both $\psi_{\ell,k}(0) = 1$ as well as

$$\|\psi_{\ell,k}\|_1 = \int_0^\infty e^{-\alpha y^2}\,\mathrm{d}y,$$

where α can be any constant.

We will also need the following results.

Lemma 3.4 *For $k \ge \min\left(\frac{d}{2}, 1\right)$,*

$$\delta_{\ell,k}(\alpha) \le \frac{3\sqrt{k}}{\sqrt{\alpha}}. \tag{26}$$

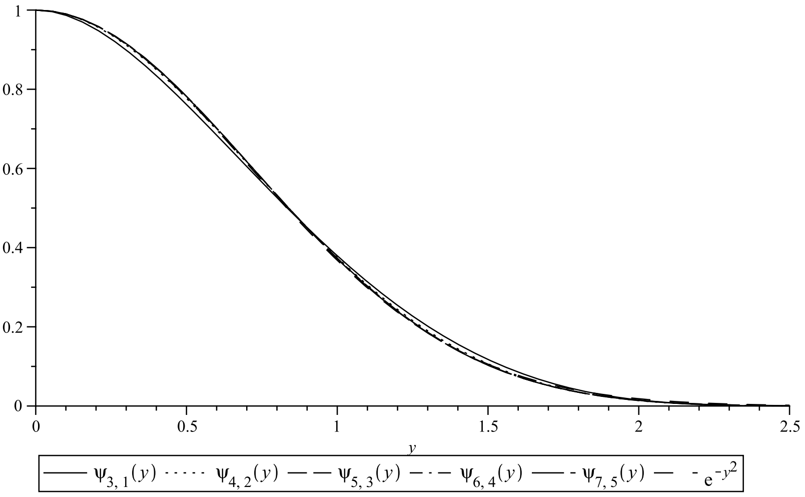

Fig. 2: The normalised equal area Wendland functions $\psi_{3,1}(y)$, $\psi_{4,2}(y)$, $\psi_{5,3}(y)$, $\psi_{6,4}(y)$,$\psi_{7,5}(y)$ with $\alpha = 1$ and $\exp(-y^2)$.

Proof From [16] we have the double inequality

$$\left(\frac{x}{x+s}\right)^{1-s} \leq \frac{\Gamma(x+s)}{x^s\,\Gamma(x)} \leq 1,$$

for $0 < s < 1$ and $x > 0$. With $s = \frac{1}{2}$ and using $\Gamma(k+1) = k\Gamma(k)$, this gives

$$\begin{aligned}
\delta_{\ell,k}(\alpha) &= \frac{(\ell+2k+1)}{2\sqrt{\alpha}} \frac{\Gamma\left(k+\frac{1}{2}\right)}{\Gamma(k+1)} \\
&\leq \frac{(\ell+2k+1)}{2\sqrt{k\,\alpha}} \\
&= \frac{\left(\lfloor \frac{d}{2}+k \rfloor + 2k + 2\right)}{2\sqrt{k\,\alpha}} \\
&\leq \frac{3\sqrt{k}}{\sqrt{\alpha}}.
\end{aligned}$$

□

Lemma 3.5 *Let* $\eta > 0$. *The function* $f_\eta : (0,\infty) \to \mathbb{R}$ *defined by*

$$f_\eta(y) := \frac{\Gamma(y+\eta)}{\Gamma(y)}, \quad y > 0, \tag{27}$$

is non-decreasing on $(0,\infty)$.

Proof We provide a proof for the convenience of the reader. Consider $F_\eta(y) := \log f_\eta(y)$. Since $f_\eta(y) > 0$ and

$$\frac{\mathrm{d}\,F_\eta(y)}{\mathrm{d}y} = \frac{1}{f_\eta(y)} \frac{\mathrm{d}\,f_\eta(y)}{\mathrm{d}y},$$

we can consider the derivative of $F_\eta(y)$ since it will have the same sign as the derivative of $f_\eta(y)$. Now

$$\frac{\mathrm{d}\,F_\eta(y)}{\mathrm{d}y} = \psi_0(y+\eta) - \psi_0(y),$$

where ψ_0 is the digamma function with the series representation [1, 6.3.16]

$$\psi_0(y+1) = -\gamma + \sum_{n=1}^{\infty} \frac{y}{n(n+y)}, \quad y \neq -1, -2, -3, \ldots$$

where γ is the Euler-Mascheroni constant. This gives

$$\frac{\mathrm{d}\,F_\eta(y)}{\mathrm{d}y} = \sum_{n=0}^{\infty} \frac{\eta}{(n+y)(n+y+\eta)},$$

which converges and is positive on $(0, \infty)$, since $\eta > 0$. □

4 Limit of the Wendland functions as $k \to \infty$

In this section we derive the limit of the normalised equal area Wendland functions as $k \to \infty$ for the original and missing Wendland functions. We start with a convergence result for the Fourier transforms.

Theorem 4.1 *Let α be a positive real constant, k be a non-negative integer or positive half-integer and $\psi_{\ell,k}$ be the normalised equal area Wendland functions defined by* (25) *with ℓ given by* (2.1)*. Then*

$$\lim_{k\to\infty} \mathcal{F}_d \psi_{\ell,k}(z) = \widehat{G}_\alpha(z) \tag{28}$$

uniformly for z in an arbitrary bounded subinterval of the positive numbers.

Proof Firstly we express the Fourier transform of $\psi_{\ell,k}$ in terms of the Fourier transform of $\tilde{\phi}_{\ell,k}$. Writing $\delta_{\ell,k}$ for $\delta_{\ell,k}(\alpha)$ and using the transformation $y = r\,\delta_{\ell,k}$ gives, from (6),

$$\begin{aligned}
\mathcal{F}_d \psi_{\ell,k}(z) &= z^{1-\frac{d}{2}} \int_0^{\delta_{\ell,k}} \psi_{\ell,k}(y)\, y^{\frac{d}{2}}\, J_{\frac{d}{2}-1}(zy)\,\mathrm{d}y \\
&= z^{1-\frac{d}{2}}\, \delta_{\ell,k} \int_0^1 \tilde{\phi}_{\ell,k}(r)\, \left(r\,\delta_{\ell,k}\right)^{\frac{d}{2}}\, J_{\frac{d}{2}-1}(z\,r\,\delta_{\ell,k})\,\mathrm{d}r \\
&= z^{1-\frac{d}{2}}\, \delta_{\ell,k}^{1+\frac{d}{2}}\, \frac{1}{(\delta_{\ell,k}\,z)^{1-\frac{d}{2}}}\, \left(\mathcal{F}_d \tilde{\phi}_{\ell,k}\right)(\delta_{\ell,k}\,z) \\
&= \delta_{\ell,k}^{d}\, \left(\mathcal{F}_d \tilde{\phi}_{\ell,k}\right)(\delta_{\ell,k} z).
\end{aligned} \tag{29}$$

Next we use Theorem 2.3 and (16) to write the Fourier transform of $\psi_{\ell,k}$ in terms of a hypergeometric function as

$$\begin{aligned}\mathcal{F}_d\psi_{\ell,k}(z) = {} & \frac{\delta_{\ell,k}^d\, 2^{-\frac{d}{2}}\Gamma(\ell+2k+1)\Gamma(k)\Gamma(d+2k)}{\Gamma(2k)\Gamma\left(\frac{d}{2}+k\right)\Gamma(\ell+d+2k+1)} \times \\ & {}_1F_2\left(\frac{d+1}{2}+k; \frac{\ell+d+2k+1}{2}, \frac{\ell+d+2k+2}{2}; -\frac{\delta_{\ell,k}^2 z^2}{4}\right), \end{aligned} \tag{30}$$

with $\delta_{\ell,k} = \delta_{\ell,k}(\alpha)$. Then the equivalent series representation is as follows

$$\begin{aligned}\mathcal{F}_d\psi_{\ell,k}(z) &= 2^{-\frac{d}{2}} \sum_{n=0}^{\infty} \frac{\Gamma(d+2k+2n)\Gamma(\ell+2k+1)\Gamma(k)}{\Gamma(2k)\Gamma(\ell+2k+1+d+2n)\Gamma\left(k+\frac{d}{2}+n\right)}\, \delta_{\ell,k}^{d+2n} \frac{\left(-\frac{z^2}{4}\right)^n}{n!} \\ &= 2^{-\frac{d}{2}} \sum_{n=0}^{\infty} w_n(k) \left(-\frac{z^2}{4}\right)^n, \end{aligned} \tag{31}$$

where

$$w_n(k) := \frac{\Gamma(d+2k+2n)\Gamma(\ell+2k+1)\Gamma(k)}{\Gamma(2k)\Gamma(\ell+2k+1+d+2n)\Gamma\left(k+\frac{d}{2}+n\right)}\, \delta_{\ell,k}^{d+2n}. \tag{32}$$

To interchange the limit as $k \to \infty$ and the infinite sum, we need to prove that this sum is dominated by an absolutely convergent series (Lebesgue's dominated convergence theorem). Using (9) twice together with Lemma 3.4 and the bound [5, 5.6.8]

$$\frac{\Gamma(x+a)}{\Gamma(x+b)} \le \frac{1}{x^{b-a}}, \quad x > 0, b-a \ge 1, a \ge 0, \tag{33}$$

we have for $k \ge 1$

$$\begin{aligned} w_n(k) &= \frac{2^{d+2n}\Gamma\left(\frac{d}{2}+k+n+\frac{1}{2}\right)\Gamma(\ell+2k+1)}{\Gamma\left(k+\frac{1}{2}\right)\Gamma(\ell+2k+1+d+2n)} \frac{\delta_{\ell,k}^{d+2n}}{n!} \\ &\le \frac{2^{d+2n}\Gamma\left(\frac{d}{2}+\frac{3k}{2}+n\right)\Gamma(3k)}{\Gamma\left(\frac{3k}{2}\right)\Gamma(3k+d+2n)} \frac{\delta_{\ell,k}^{d+2n}}{n!} \\ &= \frac{2^{d+2n}\Gamma\left(\frac{d}{2}+\frac{3k}{2}+n\right) 2^{3k-1}\Gamma\left(\frac{3k}{2}\right)\Gamma\left(\frac{3k+1}{2}\right)}{\Gamma\left(\frac{3k}{2}\right) 2^{3k+d+2n-1}\Gamma\left(\frac{3k+d}{2}+n\right)\Gamma\left(\frac{3k+d+1}{2}+n\right)} \frac{\delta_{\ell,k}^{d+2n}}{n!} \\ &= \frac{\Gamma\left(\frac{3k+1}{2}\right)}{\Gamma\left(\frac{3k+d+1}{2}+n\right)} \frac{\delta_{\ell,k}^{d+2n}}{n!} \\ &\le \frac{1}{\left(\frac{3k}{2}\right)^{\frac{d}{2}+n}} \left(\frac{3\sqrt{k}}{\sqrt{\alpha}}\right)^{d+2n} \frac{1}{n!} \\ &= \left(\frac{6}{\alpha}\right)^{\frac{d}{2}+n} \frac{1}{n!} \\ &=: U_n, \end{aligned}$$

where for the inequalities above we used

$$\frac{\Gamma(\ell+2k+1)}{\Gamma(\ell+2k+1+d+2n)} \leq \frac{\Gamma(3k)}{\Gamma(3k+d+2n)}$$

and for $k \geq 1$

$$\frac{\Gamma\left(\frac{d}{2}+k+n+\frac{1}{2}\right)}{\Gamma\left(k+\frac{1}{2}\right)} \leq \frac{\Gamma\left(\frac{d}{2}+\frac{3k}{2}+n\right)}{\Gamma\left(\frac{3k}{2}\right)},$$

both of which follow from Lemma 3.5.

The ratio test shows that $\sum_n U_n \left(-\frac{z^2}{4}\right)^n$ is absolutely convergent. Therefore we can take the limit as $k \to \infty$ inside the infinite sum, giving

$$\lim_{k\to\infty} \mathcal{F}_d\psi_{\ell,k}(z) = 2^{-\frac{d}{2}} \sum_{n=0}^{\infty} \lim_{k\to\infty} w_n(k) \left(-\frac{z^2}{4}\right)^n .$$

Using the following asymptotic result from [5]

$$\frac{\Gamma(x+a)}{\Gamma(x+b)} \sim x^{a-b}, \tag{34}$$

we can see that

$$\lim_{k\to\infty} w_n(k) = \frac{1}{n!\alpha^{\frac{d}{2}+n}}$$

and hence

$$\begin{aligned}\lim_{k\to\infty} \mathcal{F}_d\psi_{\ell,k}(z) &= (2\alpha)^{-\frac{d}{2}} \sum_{n=0}^{\infty} \frac{\left(-\frac{z^2}{4\alpha}\right)^n}{n!} \\ &= (2\alpha)^{-\frac{d}{2}}\, e^{-\frac{z^2}{4\alpha}} \\ &= \widehat{G}_\alpha(z),\end{aligned}$$

which proves pointwise convergence. Uniform convergence follows since the interval is bounded. □

Before we consider convergence of $\psi_{\ell,k}$ we establish the following technical lemma.

Lemma 4.2 *For arbitrary* $\alpha > 0$,

$$\int_0^\infty \mathcal{F}_d\psi_{\ell,k}(z)\, z^{d-1}\,\mathrm{d}z = \int_0^\infty \widehat{G}_\alpha(z)\, z^{d-1}\,\mathrm{d}z = 2^{\frac{d}{2}-1}\Gamma\left(\frac{d}{2}\right),$$

where ℓ *is given by* (2.1).

Proof From [12, 8.4.48.1], we have the following identity

$$\int_0^\infty t^{s-1}{}_1F_2(a;b_1,b_2;-t)\,\mathrm{d}t = \frac{\Gamma(s)\Gamma(a-s)\Gamma(b_1)\Gamma(b_2)}{\Gamma(a)\Gamma(b_1-s)\Gamma(b_2-s)},$$
$$0<\mathrm{Re}(s)<\min\left(\frac{1}{2}(b_1+b_2-a)+\frac{1}{4},a\right). \tag{35}$$

In our case, (35) is valid at least for $k>d$ since then

$$\min\left(\frac{1}{2}\left(\ell+\frac{d}{2}+k+1\right),\frac{d+1}{2}+k\right)>d.$$

We can calculate the integral of $\mathcal{F}_d\psi_{\ell,k}$ over the real half-line as follows. We use (9) again, and with the change of variable $w=\frac{\delta_{\ell,k}^2 z^2}{4}$ in the second step we see that

$$\begin{aligned}
\int_0^\infty \mathcal{F}_d\psi_{\ell,k}(z)\,z^{d-1}\mathrm{d}z &= \frac{\delta_{\ell,k}^d\,2^{-\frac{d}{2}}\Gamma(\ell+2k+1)\Gamma(k)\Gamma(d+2k)}{\Gamma(2k)\Gamma\left(\frac{d}{2}+k\right)\Gamma(\ell+d+2k+1)}\\
&\quad\times\int_0^\infty {}_1F_2\left(\frac{d+1}{2}+k;\frac{\ell+d+2k+1}{2},\frac{\ell+d+2k+2}{2};-\frac{\delta_{\ell,k}^2z^2}{4}\right)z^{d-1}\mathrm{d}z\\
&= \frac{\delta_{\ell,k}^d\,2^{-\frac{d}{2}}\Gamma(\ell+2k+1)\Gamma(k)\Gamma(d+2k)}{\Gamma(2k)\Gamma\left(\frac{d}{2}+k\right)\Gamma(\ell+d+2k+1)}\frac{2^{d-1}}{\delta_{\ell,k}^d}\\
&\quad\times\int_0^\infty {}_1F_2\left(\frac{d+1}{2}+k;\frac{\ell+d+2k+1}{2},\frac{\ell+d+2k+2}{2};-w\right)w^{\frac{d}{2}-1}\mathrm{d}w\\
&= \frac{2^{\frac{d}{2}-1}\Gamma(\ell+2k+1)\Gamma(k)\Gamma(d+2k)}{\Gamma(2k)\Gamma\left(\frac{d}{2}+k\right)\Gamma(\ell+d+2k+1)}\frac{\Gamma\left(\frac{d}{2}\right)\Gamma\left(k+\frac{1}{2}\right)\Gamma\left(\frac{\ell+d+2k+1}{2}\right)\Gamma\left(\frac{\ell+d+2k+2}{2}\right)}{\Gamma\left(\frac{d+1}{2}+k\right)\Gamma\left(\frac{\ell+2k+1}{2}\right)\Gamma\left(\frac{\ell+2k+2}{2}\right)}\\
&= \frac{2^{\frac{d}{2}-1}\Gamma(\ell+2k+1)\Gamma(d+2k)}{\Gamma(2k)\Gamma(\ell+d+2k+1)}\frac{\Gamma\left(\frac{d}{2}\right)2^{1-2k}\sqrt{\pi}\Gamma(2k)2^{-\ell-d-2k}\sqrt{\pi}\Gamma(\ell+d+2k+1)}{2^{1-d-2k}\sqrt{\pi}\Gamma(d+2k)\,2^{-\ell-2k}\sqrt{\pi}\Gamma(\ell+2k+1)}\\
&= 2^{\frac{d}{2}-1}\,\Gamma\left(\frac{d}{2}\right).
\end{aligned}$$

The result for $\int_0^\infty \widehat{G}_\alpha(z)\,z^{d-1}\,\mathrm{d}z$ follows from Equation (3.326.1) in [9]. □

We are now ready to state the main result.

Theorem 4.3 *Let α be a positive real constant, k be a non-negative integer or half-integer and $\psi_{\ell,k}$ be the normalised equal area Wendland functions defined by* (25) *with ℓ given by* (2.1)*. Then*

$$\lim_{k\to\infty}\psi_{\ell,k}(y)=G_\alpha(y) \tag{36}$$

with the convergence being uniform for $y\in[0,\infty)$.

Proof It follows from (7) that for a fixed y

$$|\psi_{\ell,k}(y) - G_\alpha(y)| = y^{1-\frac{d}{2}} \left| \int_0^\infty \Big(\mathcal{F}_d \psi_{\ell,k}(z) - \widehat{G}_\alpha(z) \Big) z^{\frac{d}{2}} J_{\frac{d}{2}-1}(yz) \, \mathrm{d}z \right|$$
$$\le \frac{2^{1-\frac{d}{2}}}{\Gamma(\frac{d}{2})} \int_0^\infty |\mathcal{F}_d \psi_{\ell,k}(z) - \widehat{G}_\alpha(z)| z^{d-1} \, \mathrm{d}z, \qquad (37)$$

where we have used the following bound on the Bessel function [5, 10.14.4]

$$|J_v(x)| \le \frac{|\frac{x}{2}|^v}{\Gamma(v+1)}, \quad v \ge -\frac{1}{2}, \quad x \in \mathbb{R}.$$

Since the right hand side of (37) is independent of y, the result follows if we can show that

$$D_{\alpha,k} := \int_0^\infty |\mathcal{F}_d \psi_{\ell,k}(z) - \widehat{G}_\alpha(z)| z^{d-1} \, \mathrm{d}z \to 0 \quad \text{as} \quad k \to \infty.$$

Now for arbitrary $Z > 0$ we have, because $\mathcal{F}_d \psi_{\ell,k}$ and $\widehat{G}_\alpha$ are non-negative,

$$\begin{aligned} D_{\alpha,k} &\le \int_0^Z |\mathcal{F}_d \psi_{\ell,k}(z) - \widehat{G}_\alpha(z)| z^{d-1} \, \mathrm{d}z + \int_Z^\infty \mathcal{F}_d \psi_{\ell,k}(z) \, z^{d-1} \, \mathrm{d}z + \int_Z^\infty \widehat{G}_\alpha(z) \, z^{d-1} \, \mathrm{d}z \\ &= \int_0^Z |\mathcal{F}_d \psi_{\ell,k}(z) - \widehat{G}_\alpha(z)| z^{d-1} \, \mathrm{d}z + \int_0^Z \Big(\widehat{G}_\alpha(z) - \mathcal{F}_d \psi_{\ell,k}(z) \Big) z^{d-1} \, \mathrm{d}z \\ &\qquad\qquad + 2 \int_Z^\infty \widehat{G}_\alpha(z) \, z^{d-1} \, \mathrm{d}z \\ &\le 2 \int_0^Z |\mathcal{F}_d \psi_{\ell,k}(z) - \widehat{G}_\alpha(z)| z^{d-1} \, \mathrm{d}z + 2 \int_Z^\infty \widehat{G}_\alpha(z) \, z^{d-1} \, \mathrm{d}z, \qquad (38) \end{aligned}$$

where in the second step we have used Lemma 4.2.

Given an arbitrary $\epsilon > 0$, we now choose Z sufficiently large to ensure that

$$\int_Z^\infty \widehat{G}_\alpha(z) \, z^{d-1} \, \mathrm{d}z < \frac{\epsilon}{4}.$$

For the first term in (38), we note that from Theorem 4.1, the integrand converges to zero uniformly for z in a bounded interval, thus there exists $k_1 \in \mathbb{N}$ such that

$$\int_0^Z |\mathcal{F}_d \psi_{\ell,k}(z) - \widehat{G}_\alpha(z)| z^{d-1} \, \mathrm{d}z < \frac{\epsilon}{4} \qquad \forall \quad k \ge k_1,$$

and hence

$$D_{\alpha,k} < \frac{\epsilon}{2} + \frac{\epsilon}{2} = \epsilon$$

for all $k \ge k_1$, which completes the proof. □

An interpretation of Theorem 4.3 in terms of probability distributions is that

$$\lim_{k\to\infty} \frac{1}{\sqrt{2\,\pi}\,\sigma} \tilde{\phi}_{\ell,k}\left(\frac{y}{\delta_{\ell,k}\left(\frac{1}{2\sigma^2}\right)}\right) = \frac{1}{\sqrt{2\,\pi}\,\sigma} \exp\left(-\frac{y^2}{2\sigma^2}\right), \quad y \geq 0 \tag{39}$$

where the limit on the right hand side is the right half of the Gaussian probability density with mean 0 and variance σ^2.

We note that since

$$\delta_{\ell,k}(\alpha) \sim \frac{3}{2}\sqrt{\frac{k}{\alpha}}, \tag{40}$$

from (34), we could have used the right hand side of this expression instead of $\delta_{\ell,k}(\alpha)$ to define a change of variable to study the limiting case.

5 Numerical results

In this section we present numerical results regarding the differences between the appropriately scaled Wendland functions and the Gaussian limit established in Theorem 4.3. We also consider an interpolation example using both the normalised Wendland functions $\tilde{\phi}_{\ell,k}$ and the normalised equal area Wendland functions $\psi_{\ell,k}$.

5.1 Difference with the limiting Gaussian

Let the differences between the normalised equal area Wendland functions and the limiting Gaussian be

$$E_{\ell,k}(y) := \psi_{\ell,k}(y) - \exp(-\alpha y^2)$$

and let

$$\epsilon_{\ell,k} := \sup_{y\geq 0} \left| E_{\ell,k}(y) \right|.$$

Note that the change of variable used to define $\psi_{\ell,k}$ depends on the parameter α. Figure 3 shows plots of $E_{\ell,k}(y)$ with $\alpha = 1$. The upper plots are for $d = 2$ and $k = 1.5$ and $k = 5.5$ and the lower plots are for $d = 3$ and $k = 2$ and $k = 6$.

In the absence of theoretical rates of convergence, we show numerical results. Figure 4 shows $\epsilon_{\ell,k}$ with $\alpha = 1$ for $k = 1, \ldots, 50$ and $d = 3$, 5, 7 and 9 for the original Wendland functions. Figure 5 shows $\epsilon_{\ell,k}$ with $\alpha = 1$ for $k = 0.5, \ldots, 49.5$ and $d = 2$, 4, 6 and 8 for the missing Wendland functions. Since α is just a scaling factor, the results do not vary in an essential way for different values of α.

In all cases, we see rapid convergence of $\epsilon_{\ell,k}$ to zero as the smoothness parameter k increases. This is consistent with the theoretical convergence results. Note that $\epsilon_{\ell,k}$ is not monotonically decreasing in k. We also remark that $\epsilon_{\ell,k}$ is reached at different values of y as k increases.

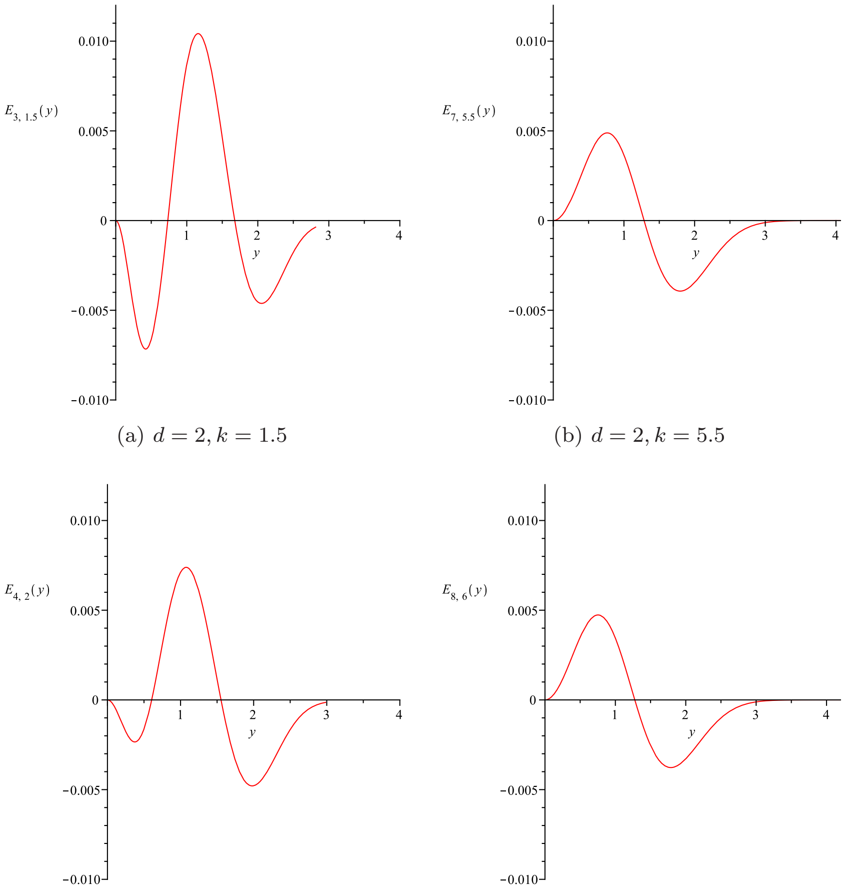

(a) $d = 2, k = 1.5$ (b) $d = 2, k = 5.5$

(c) $d = 3, k = 2$ (d) $d = 3, k = 6$

Fig. 3: $E_{\ell,k}(y)$ with $\alpha = 1$ and $0 \leq y \leq \delta_{\ell,k}(1)$. Subplots (a) and (b) are for the missing Wendland functions and subplots (c) and (d) are for the original Wendland functions.

5.2 An interpolation example

We consider an example, in which we show results obtained with both the normalised Wendland functions $\tilde{\phi}_{\ell,k}$ and the normalised equal area Wendland functions $\psi_{\ell,k}$ for different values of k. The aim of the example is to approximate the 2-dimensional Franke function [6, p.20] on $[0,5]^2$. For $k = 1,\ldots,5$ we consider interpolation as in (1) and (2), using the normalised Wendland functions $\tilde{\phi}_{\ell,k}$ and the normalised equal area Wendland functions $\psi_{\ell,k}$ with $\alpha = 2$. We use 9×9 and 17×17 equally spaced grids as the centres. The number of centres is thus $N = 81$ and $N = 289$. The L_2 error was estimated using Gaussian quadrature with a 120×120 tensor product grid of Gauss-Legendre points and the L_∞ error was estimated by using a 360×360 equally spaced grid. Table 3 shows the L_2 and L_∞

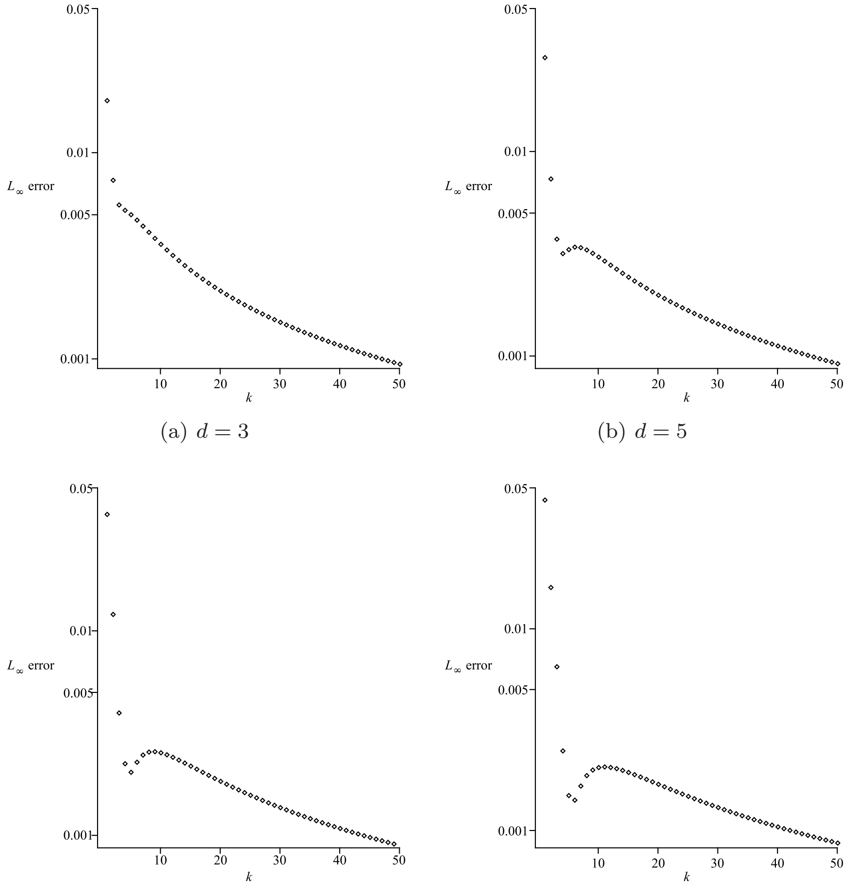

(a) $d = 3$

(b) $d = 5$

(c) $d = 7$

(d) $d = 9$

Fig. 4: $\epsilon_{\ell,k}$ on a logarithmic scale with $\alpha = 1$, $k = 1, \ldots, 50$ and $d = 3, 5, 7, 9$ for the original Wendland functions.

errors, as well as the 2-norm condition numbers of the interpolation matrices. We also show the results with the limiting Gaussian of $\exp(-2\,y^2)$, denoted by $k = \infty$.

We see from the right-hand part of Table 3 that once the argument is properly scaled to give approximately constant effective support, increasing the smoothness has remarkably little effect on the error. On the other hand the condition number increases rapidly as the smoothness increases and is very large for the Gaussian limit. Taken together, these observations suggest that any benefit gained from the higher smoothness is likely to be offset by the increased condition numbers of the matrices.

The results with the normalised Wendland functions $\tilde{\phi}_{\ell,k}$ are in the left-hand part of Table 3. We can see that the condition number is decreasing as k increases, which is due to the decreasing magnitude of the non-zero elements away from the

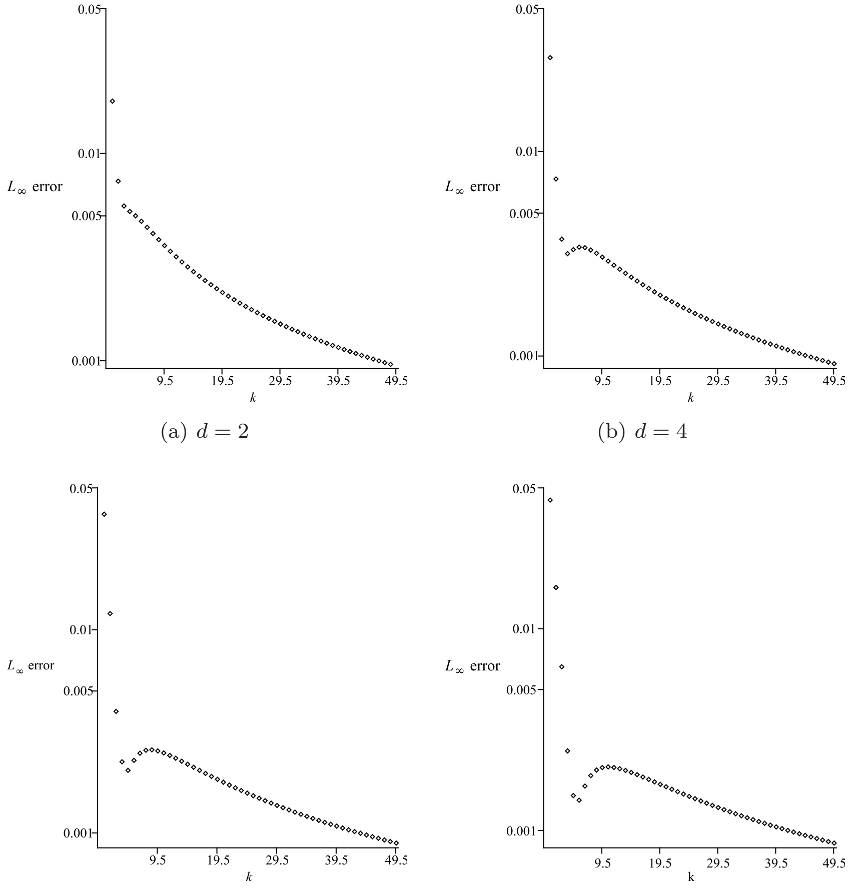

(a) $d = 2$

(b) $d = 4$

(c) $d = 6$

(d) $d = 8$

Fig. 5: $\epsilon_{\ell,k}$ on a logarithmic scale with $\alpha = 1$, $k = 0.5, \ldots, 49.5$ and $d = 2, 4, 6, 8$ for the missing Wendland functions.

diagonal. This is due to the fact that as k increases the normalised Wendland functions $\tilde{\phi}_{\ell,k}$ decay more rapidly with respect to r, as illustrated in Figure 1.

6 Conclusion

Compactly supported radial basis functions have proved very popular in scattered data approximation due to the resulting sparsity of the interpolation matrix. This paper has shown that for both the original and missing Wendland functions, the limit as the smoothness parameter goes to infinity, after suitable scaling and linear transformation, is a Gaussian RBF.

		RBF: $\tilde{\phi}_{\ell,k}$			RBF: $\psi_{\ell,k}$				
N	k	L_2 error	L_∞ error	κ	L_2 error	L_∞ error	κ	$\lambda_{\min}$	$\lambda_{\max}$
81	1	2.25e-1	6.96e-1	1.71	1.89e-1	5.89e-1	1.76e1	1.55e-1	2.74
	2	2.61e-1	7.95e-1	1.22	1.86e-1	5.78e-1	3.14e1	9.62e-2	3.02
	3	3.00e-1	8.90e-1	1.07	1.87e-1	5.79e-1	4.96e1	6.50e-2	3.22
	4	3.36e-1	9.73e-1	1.02	1.87e-1	5.80e-1	5.56e1	5.98e-2	3.30
	5	3.63e-1	1.03	1.01	1.87e-1	5.81e-1	6.37e1	5.29e-2	3.37
	∞				1.89e-1	5.89e-1	9.40e1	4.03e-2	3.78
289	1	7.75e-2	2.26e-1	4.87e1	8.20e-2	2.45e-1	4.77e2	2.25e-2	10.74
	2	7.48e-2	2.00e-1	5.64e1	7.98e-2	2.11e-1	3.89e3	3.08e-3	11.97
	3	7.47e-2	1.98e-1	3.00e1	7.88e-2	2.00e-1	1.23e4	1.04e-3	12.78
	4	7.59e-2	2.12e-1	1.24e1	7.71e-2	2.04e-1	9.88e4	1.33e-4	13.09
	5	7.75e-2	2.33e-1	6.85	7.61e-2	2.09e-1	3.77e5	3.55e-5	13.39
	∞				7.23e-2	1.90e-1	2.13e9	7.04e-9	15.00

Table 3: Results from the example in Section 5.2 showing L_2 and L_∞ errors, 2-norm condition numbers κ and minimum and maximum eigenvalues ($\lambda_{\min}$ and $\lambda_{\max}$) when using the normalised Wendland RBFs $\tilde{\phi}_{\ell,k}$ and the normalised equal area Wendland RBFs $\psi_{\ell,k}$ with $\alpha = 2$.

In Figure 1 we saw that the (original) normalised Wendland functions exhibit faster decay with respect to r as the smoothness parameter k increases. This suggests the need for a change of variable, not only to have a well-defined limit as considered in this paper, but perhaps also in practical applications. Without a change of variable, in the case of interpolation we could have a nearly diagonal interpolation matrix and consequently high errors between the interpolation points.

The number of interpolation points that fall within the support of an RBF is also related to the stationary approach to interpolation (e.g. [6, Section 12.2]), in which the goal is to keep the number of points in the support of each RBF approximately equal across different sets of centres. However here it is not the centres that are changing, but rather the basis functions that change with k.

In Figure 2 we saw the (original) normalised equal area Wendland functions, whilst formally having support $[0, \delta_{\ell,k}(\alpha)]$ that is different for each k, appear nearly identical. As a result, if the user wishes to compare the results using Wendland functions of different smoothness, the normalised equal area Wendland functions may be a more appropriate choice of RBF.

We saw in Section 5.2 that whilst the normalised equal area Wendland functions with different k might appear comparable, and give similar accuracy, the increasing support as k increases causes decreased sparsity of the interpolation matrix, and consequently an increased condition number of the linear system. This leads us to conclude that there may be little benefit from considering high values of the smoothness parameter k.

The results in the paper have illustrated the trade-off between approximation power and the condition number of the resulting linear system with Wendland functions of different smoothness. The issue of appropriate scaling and the selection of a smoothness parameter when using the Wendland functions remains a complex issue in practice.

References

1. M. Abramowitz and I. A. Stegun, *Handbook of Mathematical Functions with Formulas, Graphs and Mathematical Tables*, vol. 65 of National Bureau of Standards Applied Mathematics Series, Dover Publications, 1972.
2. G. E. Andrews, R. Askey, and R. Roy, *Special Functions*, vol. 71 of Encylopedia of Mathematics and its Applications, Cambridge University Press, Cambridge, 2000.
3. C. M. Bishop, *Pattern Recognition and Machine Learning*, Springer, 2006.
4. M. D. Buhmann, *Radial Basis Functions*, vol. 12 of Cambridge Monographs on Applied and Computational Mathematics, Cambridge University Press, Cambridge, 2003.
5. DLMF, *Digital Library of Mathematical Functions*, National Institute of Standards and Technology, 2011.
6. G. E. Fasshauer, *Meshfree Approximation Methods with MATLAB*, vol. 6 of Interdisciplinary Mathematical Sciences, World Scientific Publishing Co., Singapore, 2007.
7. M. Fornefett, K. Rohr, and H.S. Stiehl, *Radial basis functions with compact support for elastic registration of medical images*, Image and Vision Computing, 19 (2001), pp. 87–96.
8. T. Gneiting, *Radial positive definite functions generated by Euclid's hat*, Journal of Multivariate Analysis, 69 (1999), pp. 88–119.
9. I. S. Gradshteyn and I. M. Ryzhik, *Table of Integrals, Series and Products*, Elsevier, 7 ed., 2007.
10. S. Hubbert, *Closed form representations for a class of compactly supported radial basis functions*, Advances in Computational Mathematics, (2010).
11. G. Moreaux, *Compactly supported radial covariance functions*, J Geod, 82 (2008), pp. 431–443.
12. A. P. Prudnikov, Yu. A. Brychkov, and O. I. Marichev, *Integrals and Series: More Special Functions, Vol. 3*, Gordon and Breach Science Publishers, New York, 1986.
13. R. Schaback, *Creating surfaces from scattered data using radial basis functions*, in Mathematical Methods for Curves and Surfaces, M. Daehlen T. Lyche and L.L. Schumaker, eds., Vanderbilt University Press, Nashville, TN, 1995, pp. 477–496.
14. ———, *The missing Wendland functions*, Advances in Computational Mathematics, 34 (2011), pp. 67–81.
15. E.M. Stein and G. Weiss, *Introduction to Fourier Analysis on Euclidean Spaces*, vol. 32 of Princeton Mathematical Series, Princeton University Press, Princeton, New Jersey, 1971.
16. J. G. Wendel, *Note on the gamma function*, Amer. Math. Monthly, 55 (1948), pp. 563–564.
17. H. Wendland, *Piecewise polynomial, positive definite and compactly supported radial functions of minimal degree*, Advances in Computational Mathematics, 4 (1995), pp. 389–396.
18. ———, *Scattered Data Approximation*, vol. 17 of Cambridge Monographs on Applied and Computational Mathematics, Cambridge University Press, Cambridge, 2005.
19. Z. Wu, *Compactly supported positive definite radial basis functions*, Advances in Computational Mathematics, 4 (1995), pp. 283–292.
20. V. P. Zastavnyi, *On some properties of Buhmann functions*, Ukrainian Mathematical Journal, 58 (2006), pp. 1045–1067.